The Role of Curvature on Diels-Alder Functionalization of Carbon-Based Materials

B. Willocq,[a] V. Lemaur,[b] M. El Garah,[c] A. Ciesielski,[c] P. Samorì,[c] J.-M. Raquez,[a] Ph. Dubois,[a] and J. Cornil[b,*]

[a]Laboratory of Polymeric and Composite Materials (LPCM), Center of Innovation and Research in Materials and Polymers (CIRMAP), University of Mons, Place du Parc 23, B-7000 Mons, Belgium
[b]Laboratory for Chemistry of Novel Materials, Center for Research in Molecular Electronics and Photonics, University of Mons, Place du Parc 20, B-7000 Mons, Belgium
[c]ISIS & icFRC, University of Strasbourg & CNRS, 8 allée Gaspard Monge, 67000 Strasbourg, France

* E-mail: Jerome.Cornil@umons.ac.be

Supporting information

S1. Link between the parameter $d_{C\text{-}C}$ and realistic carbon-based structures

Table S1 collects the calculated values for SWNTs, DWNTs and MWNTs based on the model described in the manuscript.

Table S1. *$d_{c\text{-}c}$ obtained for realistic carbon nanotube structures*

Type of nanotube	Average diameter (nm)	Estimated $d_{c\text{-}c}$ (Å)
SWNT	1-2	9.4-11.5
DWNT	2-5	11.5-12.1
MWNT	5-50	12.1-12.25

S2. Values of $\Delta G°$ and $\Delta G^{\neq}$ for the inner attack of maleimide on PAH (M062X/6-31G(d))

The results provide evidence for a pronounced reduction of the activation barriers for more strained structures, i.e., a drop by about 20 kcal.mol^{-1} going from graphene, to multi-walled carbon nanotubes (MWNTs), double-walled carbon nanotubes (DWNTs) and single-walled carbon nanotubes (SWNTs).

Table S2. *DFT values of $\Delta G°$ and $\Delta G^{\neq}$ for the inner attack of maleimide on PAH (M062X/6-31G(d))*

$d_{c\text{-}c}$ (Å)	$\Delta G^{\neq}$ (kcal.mol^{-1})	$\Delta G°$ (kcal.mol^{-1})
12.32	39.92	31.61
12	32.84	23.10
11	26.16	11.66
10	22.67	4.55
9.32	20.30	0.05
9	19.47	-1.79
8	16.20	-8.44
7	13.04	-14.70

S3. Values of ΔG° and ΔG≠ for the inner attack of furan on PAH (M062X/6-31G(d))

The inner Diels-Alder reaction on the curved graphene sheet is illustrated in Fig. S3.a.

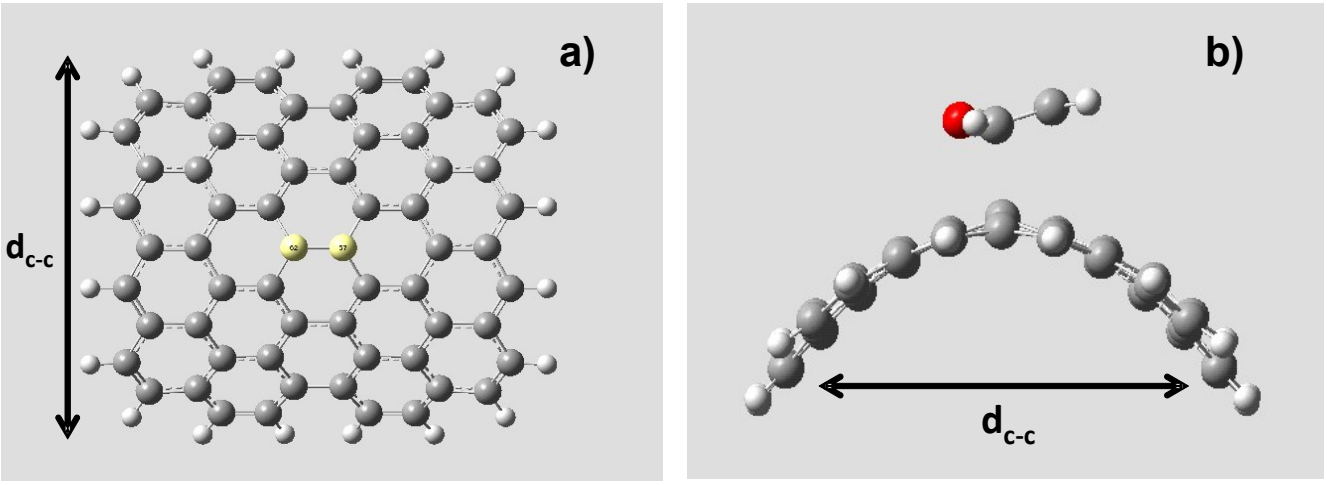

Fig. S3.a. Inner [4+2] Diels-Alder reaction on the curved graphene sheet acting as the dienophile. a) top view of the reactive site highlighted in yellow, b) side view of the furan/graphene partners involved in the Diels-Alder reaction.

The evolution of ΔG° and ΔG≠ as a function of the curvature is presented in Fig. S3.b and the corresponding data are tabulated in Table S3. As in the case of the inner attack of maleimide, the values of ΔG° and ΔG≠ also decrease with increasing curvature of the graphene sheets when the furan is involved in the reaction. However, the higher values of ΔG≠ and ΔG° point to an inefficient reaction for this diene on the core of carbon-based materials.

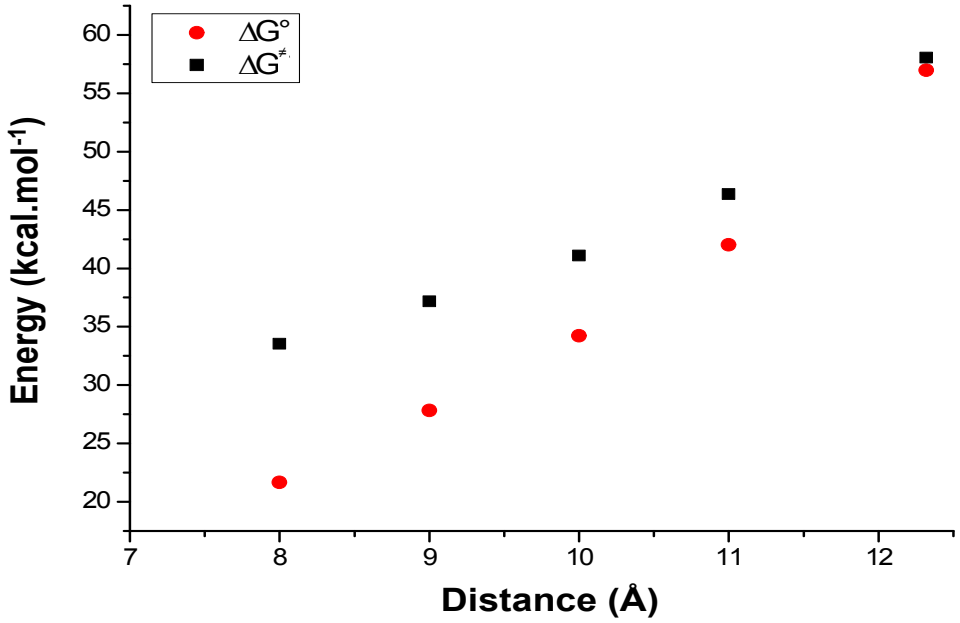

Fig. S3.b. DFT(M062X/6-31G(d))-calculated evolutions of the free energies of activation (ΔG≠) and reaction (ΔG°) for a Diels- Alder reaction involving furan and inner carbon atoms of the PAH, as a function of the curvature.

Table S3. *Values of ΔG° and ΔG≠ for the inner attack of furan on PAH (M062X/6-31G(d))*

$d_{c\text{-}c}$ (Å)	$\Delta G^{\neq}$ (kcal.mol^{-1})	$\Delta G°$ (kcal.mol^{-1})
12.32	58.04	56.98
11	46.37	42.02
10	41.09	34.22
9	37.18	27.83
8	33.53	21.66

S4. Values of ΔG° and $\Delta G^{\neq}$ for the edge attack of maleimide on PAH (M062X/6-31G(d))

Compared to the core functionalization, the trends are strikingly opposite when the edge-functionalization is considered (ΔG° and $\Delta G^{\neq}$ increase when the curvature increases).

Table S4. *Values of ΔG° and $\Delta G^{\neq}$ for the edge attack of maleimide on PAH (M062X/6-31G(d))*

$d_{c\text{-}c}$ (Å)	$\Delta G^{\neq}$ (kcal.mol^{-1})	ΔG° (kcal.mol^{-1})
12.32	24.58	-2.19
12	32.97	3.34
11	36.29	7.29
10	37.73	11.33
9	40.55	13.70
8	43.78	18.30
7	46.64	21.35

S5.a. Functionalization of SWNTs and MWNTs with fluorescent maleimide

Materials: Single-walled carbon nanotubes (Nanocyl 1100, average diameter 2nm) and multi-walled carbon nanotubes (Nanocyl 7000, average diameter 10nm) were kindly supplied by Nanocyl. DMSO and THF were purchased from VWR. N-(1-pyrenyl)maleimide was purchased from Sigma Aldrich. The functionalization of the nanotubes was performed by using the fluorescent N-(1-pyrenyl)maleimide molecule (500mg) in excess compared to the nanotube (15mg) in DMSO at 50°C during 4days, as depicted in Fig. S5. After the functionalization, the nanotubes were extensively washed by using THF, in order to wash away all physisorbed molecules, and dried for the SEM/fluorescent microscope analysis.

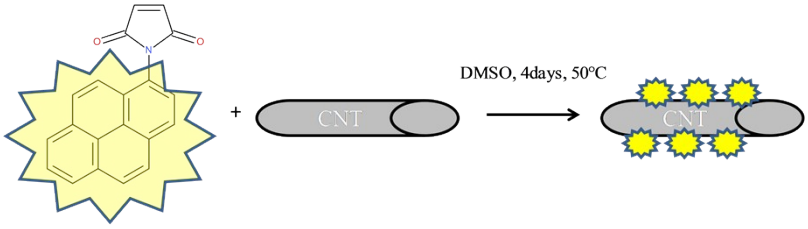

Fig. S5. Functionalization of carbon nanotubes using fluorescent N-(1-pyrenyl)maleimide

S5.b. Functionalization of SWNTs and MWNTs with non-fluorescent furan

Materials: Single-walled carbon nanotubes (Nanocyl 1100, average diameter 2nm) and multi-walled carbon nanotubes (Nanocyl 7000, average diameter 10nm) were kindly supplied by Nanocyl. DMSO and THF were purchased from VWR. Furfuryl alcohol was purchased from Sigma Aldrich. The functionalization of the nanotubes was performed as described in S.5.a. using furfuryl alcohol instead of N-(1-pyrenyl)maleimide.

S6. SEM and optical microscopy coupled with fluorescent microscopy

Carbon nanotubes were dispersed in 1,2-Dichlorobenzene (DCB) solvent. 1 mg/ml solution was sonicated using low power sonication bath for 60 minutes. The dispersion was diluted 10 times and the material was drop-casted on freshly cleaned SiO_x substrate followed by annealing at 130 °C for 120 minutes. The samples were first characterized using a FEG-Scanning electronic microscope (SEM) to show their morphological structures, then their fluorescence was recorded using a BX51 universal research microscopy. The SEM and optical microscopes mapped the same area for each material (SWNTs (Fig. S6.a) and MWNTs (Fig. S6.b). Superimposed SEM and fluorescence images shown in Fig. S6.a clearly illustrate the strong emission of SWNTs (Fig. S6.a top in SI), whereas no similar effect was observed for MWNTs (Fig. S6.a bottom in SI). Fig. S6.b highlights this effect and shows the emission difference between MWNTs and SWNTs. Note also that the materials are prepared and characterized in the same conditions.

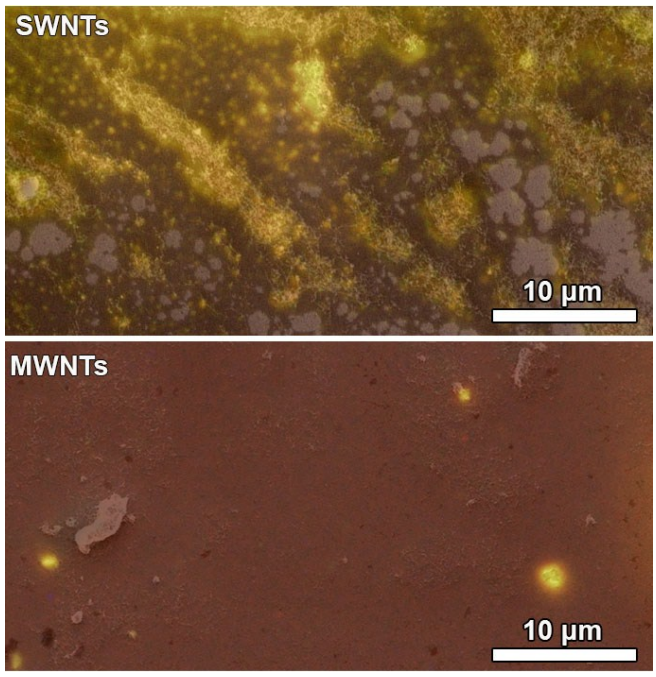

Fig. s6.a. Superimposed SEM and fluorescence images of the same areas of SWNTs (top) and MWNTs (bottom)

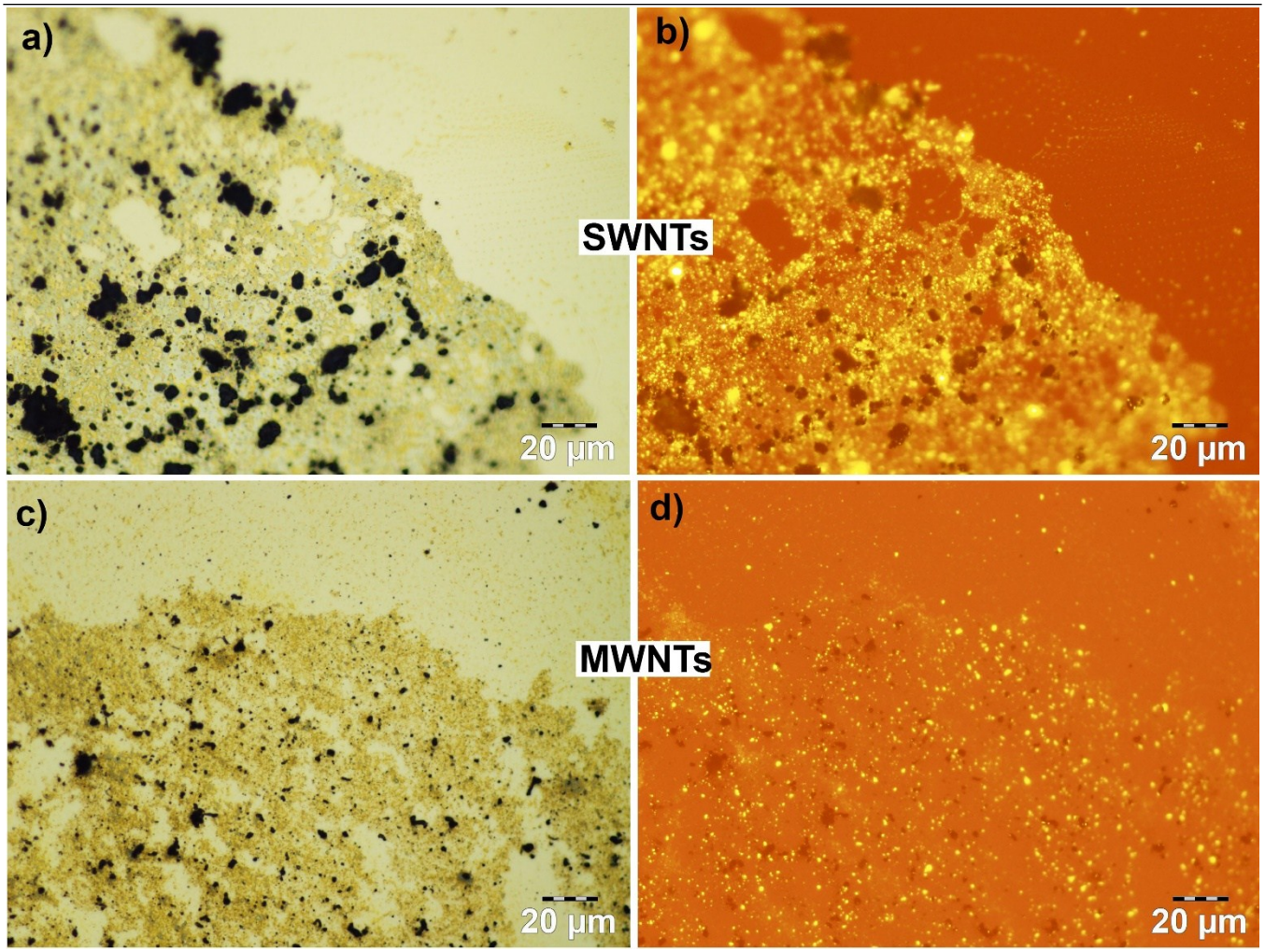

Fig. s6.b. Optical microscope and fluorescence images of MWNTs (a) and (b) respectively. Optical microscope and fluorescence images of SWNTs (c) and (d) respectively.

A Thermo Scientific K-Alpha X-ray Photoelectron Spectrometer (XPS) using monochromatic AlKα radiation (hv = 1486.6 eV) was used to investigate the chemical composition of the films. Fig. S6.c shows the decomposition of C1s spectra of MWNTs and SWNTs, using Avantage. The energies and meaning of each component are as follows: for example in the case of maleimide_MWNTs, (1)~284.07 eV corresponds to the sp^2 carbons on the nanotubes, (2)~285.03 eV corresponds to sp^3 carbon atoms, (3)~286.08 eV and (4)~288.18 eV correspond to carbon bonded to oxygen. In the case of maleimide_SWNTs, (1')~284.08 eV corresponds to sp^2 carbons of the nanotubes, (2')~284.92 eV corresponds to sp^3 carbon atoms, (3')~286.18 eV and (4')~288.08 eV correspond to carbon bonded to oxygen. The percentages of the peaks are listed in Table S6. Interestingly, XPS C1s curve shows the percentage of carbon C=C and C-C for both MWNTs and SWNTs (Fig. S6.c in SI). The decomposition of the C1s curve yields 62.75 % of C=C and 19.00 % of C-C for maleimide-MWNTs compared to 55.57 % and 32.74 % for maleimide-SWNTs, respectively. Conversely, when furan is used as reactant the functionalized MWCTs C1s curve yields 59.29 % of C=C and 14.06 % of C-C compared to 59.55 % C=C, 14.09 % of C-C when and SWCNTs are employed. The higher percentage of C-C of maleimide functionalized SWCNTs demonstrates that this nanostructure undergoes a greater chemical change compared to both MWNTs + maleimide and furan functionalized SWNTs and MWNTs.

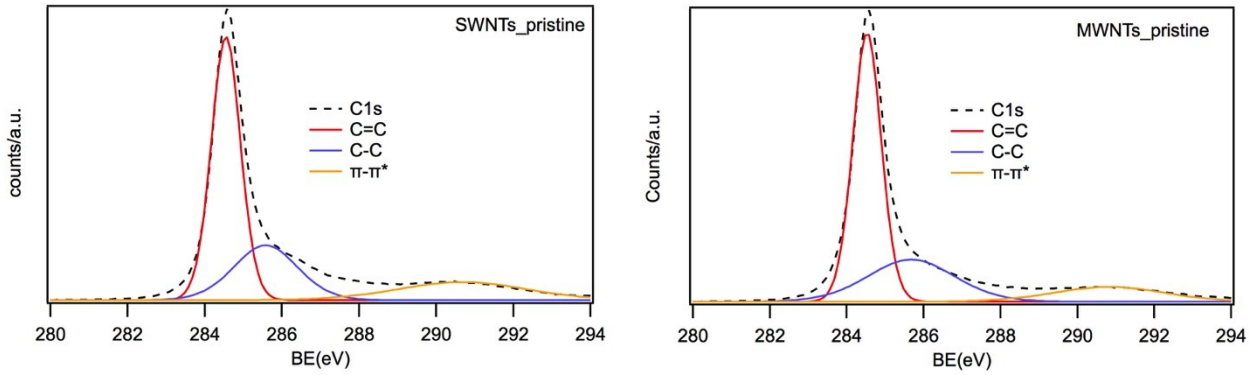

Fig. s6.c. XPS C1s of unfunctionalized MWNTs (left) and SWNTs (right).

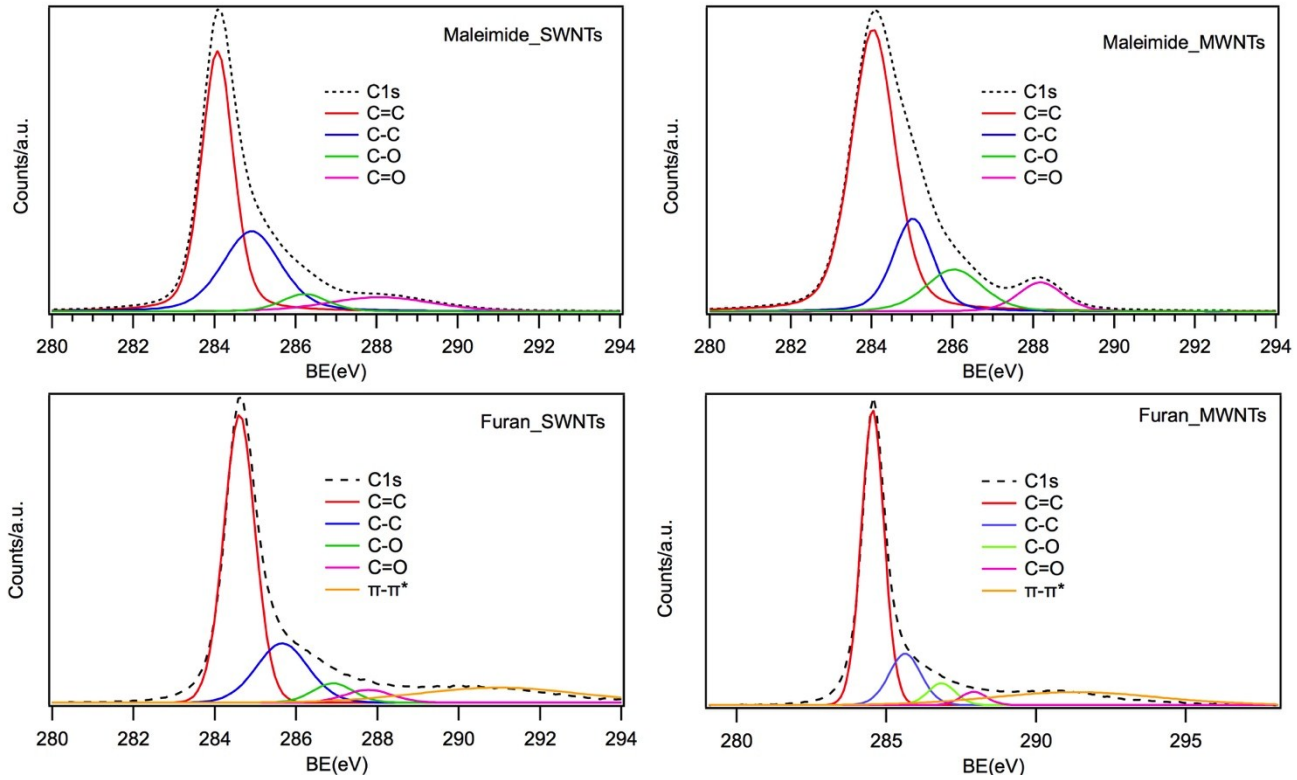

Fig. s7.c. XPS C1s of functionalized MWNTs and SWNTs with maleimide (top) and Furan (bottom)

Table S6. Detailed information of the C1s spectra, including the binding energies and percentages of functional groups

		C=C	C-C	C-O	C=O	π-π*
SWNTs_pristine	BE(eV)	284.58 ± 0.1	285.58 ± 0.1	-	-	290.68 ± 0.1
	Percentage(%)	68.16	12.84	-	-	19.01
MWNTs_pristine	BE(eV)	284.58 ± 0.1	285.58 ± 0.1	-	-	290.83 ± 0.1
	Percentage(%)	74.76	11.14			14.10
Maleimide_SWNTs	BE(eV)	284.08± 0.1	284.92± 0.1	286.18± 0.1	288.08± 0.1	-
	Percentage(%)	55.57	32.74	1.88	9.81	-
Maleimide_MWNTs	BE(eV)	284.07 ± 0.1	285.03 ± 0.1	286.08 ± 0.1	288.18 ± 0.1	-
	Percentage(%)	62.75	19.00	1.48	6.72	-
Furan_SWNTs	BE(eV)	284.68± 0.1	285.88± 0.1	286.98± 0.1	287.78± 0.1	290.98± 0.1
	Percentage(%)	59.55	14.09	7.26	3.80	15.31
Furan_MWNTs	BE(eV)	284.58± 0.1	285.63± 0.1	286.58± 0.1	287.88± 0.1	290.99± 0.1
	Percentage(%)	59.29	14.06	5.81	2.63	14.22